

## XPS Study of the Dependence on Stoichiometry and Interaction with Water of Copper and Oxygen Valence States in the $\text{YBa}_2\text{Cu}_3\text{O}_{7-x}$ Compound

P. SALVADOR\* AND J. L. G. FIERRO

*Instituto de Catálisis y Petroleoquímica, CSIC, Serrano, 119  
28006 Madrid, Spain*

AND J. AMADOR, C. CASCALES, AND I. RASINES

*Instituto de Ciencia de Materiales, CSIC, Serrano, 113-28006 Madrid, Spain*

Received November 9, 1988; in revised form March 27, 1989

In order to elucidate the valence states of both copper and oxygen in  $\text{YBa}_2\text{Cu}_3\text{O}_{7-x}$ , as a function of the oxygen content, their  $\text{O}_{1s}$  and  $\text{Cu}_{2p}$  core-level X-ray photoelectron spectra were studied at room temperature for  $0.9 \geq x \geq 0.1$ . No evidence of the  $\text{Cu}^{3+}$  (i.e.,  $3d^8$ ) configuration was found for the ground state of a superconducting sample ( $x \approx 0.1$ ). Rather, the ground state for this composition can be described as a mixture of two configurations: mainly  $3d^9KL$  (i.e.,  $\text{Cu}^{2+}-\text{O}^-$  hybridization), where  $K$  represents an electron of the conduction band and  $L$  stands for a hole in the oxygen bonded to a virtually divalent copper, and some  $3d^{10}$  (i.e.,  $\text{Cu}^+$ ). The amount of monovalent copper was found to increase with  $x$ , as oxygen ( $\text{O}^-$  species) from  $\text{Cu}_1-\text{O}$  chains parallel to the crystallographic  $b$  axis leave the lattice and electrons are transferred to the adjacent  $\text{Cu}^{2+}$  ions. Simultaneously, the concentration of holes delocalized in the oxygen valence band decreases, the Fermi level goes upward, and the material's behavior at room temperature changes from quasi-metallic (degenerated  $p$ -type semiconductor) to  $p$ -type semiconducting. For  $x \approx 0.9$  the amount of  $\text{Cu}^+$  predominates over that of  $\text{Cu}^{2+}$ . The high reactivity of the superconducting material with water is evidenced by the special characteristics of its  $\text{O}_{1s}$  core-level spectrum. The presence of  $\text{OH}^-$  ions indicates dissociative adsorption of water molecules from the air. The XPS signal due to  $\text{OH}^-$  species is higher than that of the  $\text{O}^{2-}$  lattice ions, even when the sample was preserved from exposure to air. Moreover, when the superconducting sample was contaminated by prolonged exposition to air, the  $\text{O}^{2-}$  signal could hardly be observed. These results are consistent with the existence of delocalized holes in  $\text{O}_{2p}$  orbitals. In fact, the  $\text{O}^-$  lattice species strongly react with water molecules to produce more stable  $\text{OH}^0$  radicals, which further recombine to generate  $\text{H}_2\text{O}_2$  whose decomposition is catalyzed by  $\text{Cu}^{2+}$  ions. As a result, molecular oxygen from lattice  $\text{O}^-$  species is evolved. Charge neutrality in the superconductor lattice is preserved by filling  $\text{O}^-$  vacancies with  $\text{OH}^-$  groups, which became coordinated to  $\text{Ba}^{2+}$  ions as inferred from the analysis of the  $\text{Ba}_{3d}$  XPS spectrum. © 1989 Academic Press, Inc.

### Introduction

A full understanding of the superconductivity mechanisms in the  $R\text{Ba}_2\text{Cu}_3\text{O}_{7-x}$  ( $R =$

Y, La, lanthanide) oxides requires a fair knowledge of the local electronic configuration of Cu and oxygen ions. The transition at room temperature from the semiconducting ( $x \geq 0.5$ ) to the metallic phase ( $0.5 > x > 0$ ), which shows superconductivity at temperatures near that of liquid nitrogen, is

\* To whom correspondence should be addressed.

governed by the oxygen content,  $x$ , and, therefore, by the formal oxidation state of Cu atoms. Assuming a fixed integer valence for the remaining atoms, i.e., 2 for oxygen and barium and 3 for yttrium, the formal valence for copper should be 2.3 for  $x = 0$ , 2 for  $x = 0.5$ , and 1.7 for  $x = 1$ . Therefore, a mixture of  $\text{Cu}^{2+}$  and  $\text{Cu}^{3+}$  ions should be expected for  $x < 0.5$ .

The crystal structure of  $\text{YBa}_2\text{Cu}_3\text{O}_{7-x}$  has been established by X-ray diffraction (1), neutron diffraction (2), and high-resolution transmission electron microscopy (3). The orthorhombic unit cell for  $0 \leq x \leq 0.5$  contains two copper atoms,  $\text{Cu}_2$ , with a square pyramidal coordination to 5 oxygen atoms, and one copper atom,  $\text{Cu}_1$ , surrounded by 4 oxygens in square planar coordination, forming  $\text{Cu}_1\text{-O}$  chains along the  $b$  axis. Pyramidal coordination is frequent for Cu(II); thus, the valence of  $\text{Cu}_2$  atoms is assumed to be 2. On the other hand, from neutron diffraction experiments it is now well known that the oxygen sites of the  $\text{Cu}_1\text{-O}$  chains are practically emptied when  $x$  increases from 0 to 0.5, and the orthorhombic crystal structure becomes tetragonal. In this case, it must be concluded that  $\text{Cu}_1$  atoms are progressively reduced from  $\text{Cu}^{3+}$  ( $x = 0$ ) to  $\text{Cu}^{2+}$  ( $x = 0.5$ ). Because the superconductivity decreases or even vanishes when  $x$  increases, it is inferred that the presence of  $\text{Cu}^{3+}$  at  $\text{Cu}_1$  sites is essential for superconducting properties. The valence of copper in these oxides has been investigated mainly by X-ray absorption (4–11) and photoemission (12–15). While some authors claim the existence of  $\text{Cu}^{3+}$  (4, 6, 9, 10, 14), others do not find any evidence of this valence state (5, 7, 8, 12, 13, 15). Lengeler *et al.* (11) recently concluded that  $\text{YBa}_2\text{Cu}_3\text{O}_{6.9}$  ( $x = 0.1$ ) contains two divalent  $\text{Cu}_2$  ions with a K-edge similar to those present in the green semiconductor  $\text{Y}_2\text{BaCuO}_5$ , consisting in 0.84  $\text{Cu}^{3+}$  as in  $\text{KCuO}_2$  and in 0.16  $\text{Cu}^{1+}$  as in  $\text{Cu}_2\text{O}$ . Formally,  $\text{Cu}^{3+}$  can have two different configurations

at the ground state, i.e.,  $3d^8$  and  $3d^9 L$ , where  $L$  stands for a hole in the oxygen ligand. While  $3d^8$  is characteristic of the ionic bond between copper and oxygen,  $3d^9 L$  indicates strong covalency in the Cu–O bond. The well-known electronic structure of the superconducting compound implies a strong mixing of  $\text{Cu}_{3d}$  and  $\text{O}_{2p}$  orbitals, favoring the  $3d^9 L$  configuration. Moreover, holes in the  $\text{O}_{2p}$ -derived valence band have been directly observed by core-level excitation of oxygen  $1s$  electrons into empty  $p$ -states of the Fermi level,  $E_F$ , via electron energy loss spectroscopy (16). Inverse photoemission measurements also show the existence of unoccupied  $\text{O}_{2p}$  orbitals just above the top of the valence band (17). From high-energy inelastic electron spectroscopy measurements, Kamaras *et al.* (18) have shown that the density of empty  $\text{O}_{2p}$  states close to  $E_F$  increases with  $x$ . Moreover, all spectroscopic investigations have failed to reveal pure  $3d^8$  configurations, either in  $\text{YBaCu}_2\text{O}_{7-x}$  superconducting materials or in compounds like  $\text{NaCuO}_2$  (19) and  $\text{KCu}(\text{biuret})_2$  (biuret =  $\text{NH}_2\text{CONHCONH}_2$ ) (7), where a pure formal valency of 3 is expected.

On the other hand, the existence of delocalized holes in the  $\text{O}_{2p}$  energy levels should involve the existence of stable  $\text{O}^-$  species in the superconductor lattice. This explains the unusual release of oxygen from the superconductor when it is in contact with water (20), suggesting interesting catalytic properties for these new superconducting materials, for instance in the formation of  $\text{CH}_3$  radicals from methane. However, this is far from the scope of this paper and will be considered elsewhere (21). Here we have used X-ray photoelectron spectroscopy (XPS) to study not only the dependence on  $x$  of the actual valence of copper and oxygen in  $\text{YBa}_2\text{Cu}_3\text{O}_{7-x}$  but also the effect that the interaction of the superconductor with water has on both the copper oxidation state and the lattice stability.

## Experimental

YBa<sub>2</sub>Cu<sub>3</sub>O<sub>7-x</sub> ceramics were prepared by homogeneously mixing analytical grade Y<sub>2</sub>O<sub>3</sub>, BaO<sub>2</sub>, and CuO powders. The mixture was pressed into pellets and heated to 975°C in air for 48 hr. This process was repeated twice after regrinding. The material prepared in this way was monophasic, orthorhombic, and served as the starting material for obtaining samples with three different oxygen contents via annealing treatments under controlled temperature and atmosphere (22), as indicated in Table I.

The pellets used for XPS measurements were surface cleaned by scraping them with a hard metallic knife before the annealing treatments. In order to avoid contamination of the pellets during air exposure, especially from water vapor, they were removed from the furnace at ~150°C and immediately transferred into the vacuum chamber of the XPS spectrometer under a residual pressure of ca. 10<sup>-5</sup> Torr. Conductivity measurements performed at the temperature of liquid nitrogen confirmed that the sample 4-O<sub>2</sub> was superconducting, whereas the samples 4-H<sub>2</sub> and 8-N<sub>2</sub> were not and showed *p*-type semiconducting behavior at room temperature. For comparative purposes the XPS spectra of the contaminated 4-O<sub>2</sub> sample were also studied. With this aim, the sample was left in contact with the air for several days after the

annealing treatment at 400°C in O<sub>2</sub> (see Table I).

XPS spectra were obtained with a Leybold Heraeus LHS 10 spectrometer, working in the  $\Delta E = \text{constant}$  mode at a pass energy of 20 eV. The spectrometer was provided with a hemispherical electron analyzer and a MgK $\alpha$  anode X-ray source (MgK $\alpha = 1253.6$  eV). Samples 3 mm thick were mounted on a long rod placed in an introduction chamber, and outgassed to ca. 10<sup>-5</sup> Torr for 5 min before the samples were moved into the turbopumped analysis chamber. The pressure in this chamber was maintained below  $3 \times 10^{-9}$  Torr during data acquisition. Either 20 or 50 eV energy regions of the photoelectrons of interest at the pass energy selected were chosen as a compromise, enabling acceptable energy resolution to be obtained within reasonable data acquisition times. Each spectral region was signal averaged to a number of scans to provide a good signal-to-noise ratio. Although surface charging was observed on all samples, accurate binding energies (BEs) could be determined by charge referencing with the adventitious C<sub>1s</sub> line arising from oil vapor contamination in the initial outgassing step at BE = 284.6 eV.

## Results and Discussion

### *Cu<sub>2p</sub> Core-Level Spectra and Copper Oxidation States*

Figure 1 shows the Cu<sub>2p</sub> spectra of the three samples obtained under the experimental conditions shown in Table I, with oxygen contents per formula of 6.9, 6.5, and 6.1 ( $x \approx 0.1, 0.5, 0.9$ ), respectively. The spectra of the sample 4-O<sub>2</sub>, which was exposed to the air for several days, and those of a CuO reference sample are also shown in Fig. 1.

The XPS spectrum of CuO (Fig. 1a) presents the typical Cu<sub>2p<sub>3/2</sub></sub> and Cu<sub>2p<sub>1/2</sub></sub> lines separated by 20 eV, as reported in the liter-

TABLE I

PREPARATIVE CONDITIONS AND CHARACTERISTICS OF YBa<sub>2</sub>Cu<sub>3</sub>O<sub>7-x</sub> SAMPLES<sup>a</sup> WITH DIFFERENT OXYGEN CONTENTS

Sample	Temperature (°C)	Time (hr)	Atmosphere	<i>x</i>	Present phase
4-O <sub>2</sub>	400	24	Flushing O <sub>2</sub>	~0.1	Orthorhombic
4-N <sub>2</sub>	400	24	Flushing N <sub>2</sub>	~0.5	Orthorhombic
8-N <sub>2</sub>	800	24	Flushing N <sub>2</sub>	~0.9	Tetragonal

<sup>a</sup> All the samples were heated at 2°C min<sup>-1</sup> and cooled to ~150°C at the same rate.

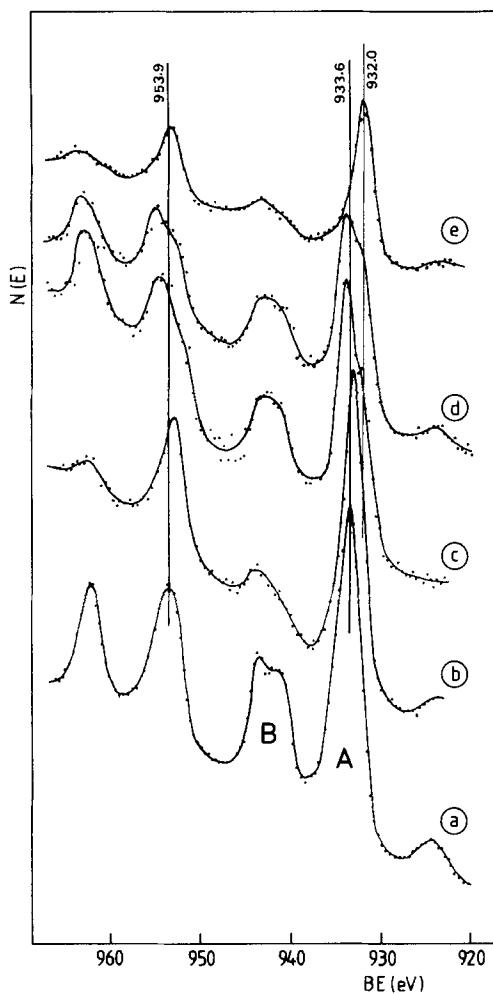


FIG. 1. Room-temperature XPS  $\text{Cu}_{2p}$  core-level spectra of the  $\text{Ba}_2\text{Cu}_3\text{YO}_{7-x}$  sample subjected to various pretreatments: (b) exposed to air at room temperature; (c) oxidized in an oxygen flow at  $400^\circ\text{C}$ ; (d) reduced in a nitrogen flow at  $400^\circ\text{C}$ ; (e) reduced in a nitrogen flow at  $800^\circ\text{C}$ . For comparative purposes, the  $\text{Cu}_{2p}$  core-level spectrum of the  $\text{CuO}$  reference compound (a) is also included. All the spectra show whole spin-orbit splitting with intense final-state satellites.

ature (23). Each core level shows two lines, *A* and *B*, which are associated with the  $2p3d^{10}L$  and  $2p3d^9$  final states, respectively (24). The *B* peak is characteristic of  $\text{Cu}^{2+}$  compounds. The  $2p3d^{10}L$  final state, where *L* stands for a ligand hole, involves charge

transfer from the  $\text{O}_{2p}$ -derived valence band levels to the  $\text{Cu}_{3d}$  orbitals. The spectra of  $\text{YBa}_2\text{Cu}_3\text{O}_{7-x}$  (Figs. 1b–1e) show important differences compared with those of  $\text{CuO}$ , and are very sensitive to the value of *x*. For the superconducting sample, i.e., the most oxidized ( $x \approx 0.1$ , Fig. 1c), the *A* peak appears shifted toward higher binding energies ( $\text{BE} = 934.1$  eV) than those in  $\text{CuO}$  ( $\text{BE} = 933.6$  eV). Moreover, an incipient shoulder centered at  $\sim 932$  eV is present. The *B/A* intensity ratio is also lower in  $\text{YBa}_2\text{Cu}_3\text{O}_{6.9}$  (0.37) than in  $\text{CuO}$  (0.49). For  $x = 0.5$  (Fig. 1d) the position of the *A* peak and the *A/B* ratio do not practically change, while the shoulder at  $\sim 932$  eV becomes more intense than that for  $x = 0.1$ . Finally, for  $x = 0.9$  (Fig. 1e) the *A* peak almost disappears (only a small shoulder can be observed) and the shoulder appearing at  $\sim 932$  eV for  $\approx 0.5$  and  $x = 0.1$  becomes a well-defined peak. Moreover, the *B* peak decreases considerably.

It is especially interesting to compare the spectrum of the orthorhombic superconducting sample,  $\text{YBa}_2\text{Cu}_3\text{O}_{6.9}$  (Fig. 1c), with that corresponding to its air-exposed counterpart (Fig. 1b). Three main features characterize the spectrum of the latter: (a) the setting of the *A* peak at  $\text{BE} = 933.4$  eV, very near that corresponding to the  $\text{Cu}$  spectrum; (b) the disappearance of the shoulder at  $\text{BE} \approx 932$  eV; and (c) the lowering of the intensity of the  $2p3d^9$  final state (*B* peak), which gives a ratio  $B/A = 0.2$ , considerably lower than that for the non-contaminated sample ( $B/A = 0.37$ ). Table II summarizes the main spectral features of the different XPS spectra.

According to recent X-ray absorption results reported by Lengeler *et al.* (11), the superconductor  $\text{YBa}_2\text{Cu}_3\text{O}_{6.9}$  contains two  $\text{Cu}^{2+}$  ions per formula, with a *K*-edge similar to that of semiconducting  $\text{Y}_2\text{BaCuO}_5$  but different from that in  $\text{CuO}$ , which contains 0.84  $\text{Cu}^{3+}$  ions, like those present in  $\text{KCuO}_2$ , and 0.16  $\text{Cu}^+$  ions as in  $\text{Cu}_2\text{O}$ . Like

TABLE II  
BINDING ENERGIES<sup>a</sup> (eV) OF SEVERAL ATOMIC LEVELS

Sample	Pretreatment	O <sub>1s</sub>	Ba <sub>4d</sub>		Cu <sub>2p</sub>	
			3/2	5/2	1/2	3/2
Ba <sub>2</sub> Cu <sub>3</sub> YO <sub>7-x</sub>	None	531.2 (528.7)	795.8	780.6	953.3	933.4
Ba <sub>2</sub> Cu <sub>3</sub> YO <sub>7-x</sub>	Oxidized in O <sub>2</sub> at 400°C	532.0 (530.3)	795.4	779.6	954.3	934.1 (932.0)
Ba <sub>2</sub> Cu <sub>3</sub> YO <sub>7-x</sub>	Annealed in N <sub>2</sub> at 400°C	531.9 (530.5)	795.0	779.1	954.6	934.1 (932.0)
Ba <sub>2</sub> Cu <sub>3</sub> YO <sub>7-x</sub>	Annealed in N <sub>2</sub> at 800°C	532.3 (530.0)	794.6	777.8	952.3	931.8 (934)
CuO	None	(531.5) 529.5	—	—	953.9	933.6

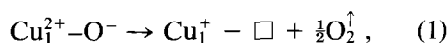
Note. BE of less intense lines are indicated in parentheses.

<sup>a</sup> Referenced to C<sub>1s</sub> line at BE = 284.6 eV.

other authors, Lengeler *et al.* (11) think that Cu<sup>2+</sup> ions should occupy Cu<sub>2</sub> sites in the orthorhombic unit cell, while Cu<sup>3+</sup> and Cu<sup>1+</sup> probably occupy Cu<sub>1</sub> sites. Also according to Lengeler *et al.* (11), the formal trivalency of copper in the superconductor cannot be understood as actual Cu<sup>3+</sup> with 3d<sup>8</sup> ground-state configuration, but rather as a valence state represented by the configuration Cu<sub>3d<sup>9</sup>O<sub>2p<sup>5</sup></sub>. Therefore, the main difference between this configuration and that of formal Cu<sub>3d<sup>9</sup>O<sub>2p<sup>6</sup></sub> is the existence of a hole in the ligand O<sub>2p</sub>-derived band. Bianconi *et al.* (13) have studied the differences between the XPS Cu<sub>2p</sub> spectrum of the di- and trivalent copper compounds K<sub>2</sub>Cu<sup>2+</sup>(biuret)<sub>2</sub> and KCu<sup>3+</sup>(biuret)<sub>2</sub>, respectively, and have not found evidence of Cu<sup>3+</sup> ions with 2p3d<sup>8</sup> final states in the trivalent compound. On the other hand, the main difference between both spectra lies in the shape of the B peak associated with the 2p<sub>3/2</sub>3d<sup>9</sup> final state in the divalent copper compound, and the 2p<sub>3/2</sub>3d<sup>9</sup>L final state corresponding to the 3d<sup>9</sup>L configuration in the ground state for the trivalent compound. Steiner *et al.* (19) compared the XPS Cu<sub>2p<sub>3/2</sub></sub> spectra of NaCuO<sub>2</sub>, with formally Cu<sup>3+</sup> ions, and those of CuO. They found that the peak intensity ratios A/B increased considerably in the trivalent compound, while the BE of</sub></sub>

the 2p3d<sup>10</sup>L<sup>2</sup> final state (A peak in NaCuO<sub>2</sub>) was about 1.5 eV higher than that of the 2p3d<sup>10</sup>L final state (A peak in CuO).

On the basis of these statements, the spectral features of Fig. 1 can be interpreted as follows. The existence of Cu<sup>2+</sup> ions in the sample of YBa<sub>2</sub>Cu<sub>3</sub>O<sub>6.9</sub> (Fig. 1c) is confirmed by the presence of a relatively high B peak at BE ≈ 942 eV, associated with the 2p3d<sup>9</sup> final-state configuration. However, the appearance of the A peak at a BE = 934.1 eV, higher than in CuO, seems to indicate that some Cu<sup>2+</sup> ions with a Cu<sub>3d<sup>9</sup>O<sub>2p<sup>5</sup></sub> configuration in the ground state are also present. Moreover, the incipient shoulder at a BE ≈ 932 eV reveals the existence of a very small proportion of Cu<sup>+</sup> ions. This could be expected taking into account that oxygen vacancies are generated at the Cu<sub>1</sub>-O chains as x increases. In fact, the release of O<sup>-</sup> species coordinated to Cu<sub>1</sub> atoms in the Cu<sub>1</sub>-O chains parallel to the b axis should be accompanied by the reduction of the copper ions, according to</sub>



where  $\square$  represents an O<sup>-</sup> vacancy.

In the ideal superconducting sample (x = 0), all the oxygen positions in the Cu<sub>1</sub>-O chains are filled and the material behaves like a metal (degenerated p-type semicon-

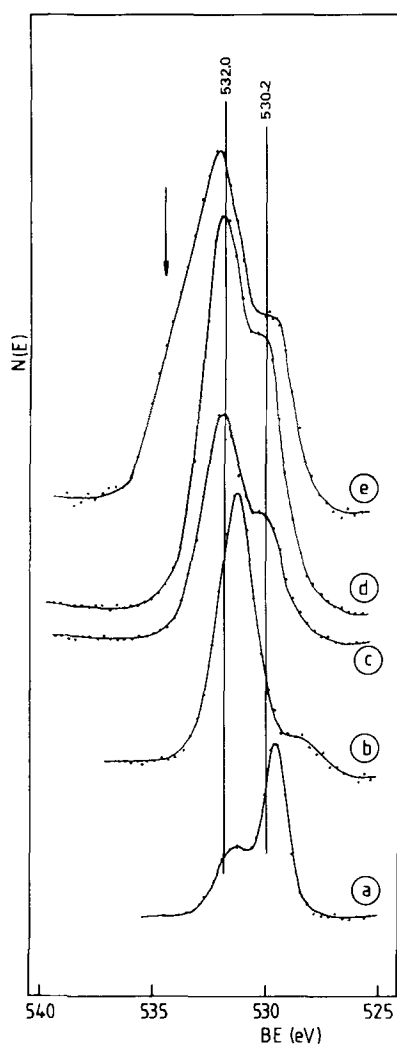


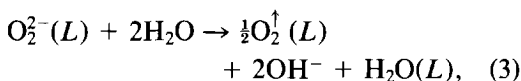
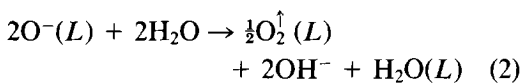
FIG. 2. Room-temperature XPS  $\text{O}_{1s}$  core-level spectra of the  $\text{YBa}_2\text{Cu}_3\text{O}_{7-x}$  sample subjected to the same pretreatments as in Fig. 1.

ductor) at room temperature. The predominance of the electronic configuration  $3d^9L$  in this case produces, as already stated, a downward shift of the Fermi level, which invades the  $\text{O}_{2p}$  valence band. The oxygen energy levels below  $E_F$  then become empty (holes associated with  $\text{O}^-$  species) and form a thin band for conduction of thermally excited electrons from the filled energy level below  $E_F$ . When  $x$  increases,  $\text{O}^-$  vacancies

are generated and electrons are transferred from  $\text{O}^-$  sites to adjacent copper ions, as Eq. (1) indicates. In this way, copper decreases its valence state and reaches the  $3d^{10}$  configuration. At the same time the number of holes in the upper part of the  $\text{O}_{2p}$ -derived valence band drastically diminishes and  $E_F$  moves up. At  $x \geq 0.5$  the material reaches the electronic configuration typical of a  $p$ -type semiconductor, with  $E_F$  just above the upper limit of the valence band, and loses its superconducting properties.

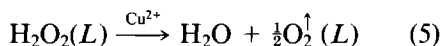
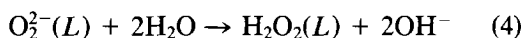
Figure 2 shows the  $\text{O}_{1s}$  core-level spectra for the same samples as in Fig. 1. A well-defined couple of peaks characterize these spectra at binding energies of  $\approx 530$  and  $\approx 532$  eV, respectively. The exact position and relative intensity of both peaks strongly depend on the sample (see Table II). According to literature data about  $1s$  core-level spectra in metal oxides, the lower binding energy peak corresponds to species with two negative charges,  $\text{O}^{2-}$ , while the higher energy peak is associated with oxygen species having only one negative charge, which include  $\text{O}^-$ ,  $\text{O}_2^-$ , and  $\text{OH}^-$  species (25). In the case of  $\text{CuO}$ , the higher BE peak at 351.5 eV is due to hydroxyl groups resulting from the dissociative adsorption of water molecules. This peak is considerably less intense than that associated with  $\text{O}^{2-}$  species appearing at lower BE which indicates a relatively weak surface hydration of  $\text{CuO}$ . This is not the case for the  $\text{YBa}_2\text{Cu}_3\text{O}_{7-x}$  samples, in which the higher BE peak is much more intense than that at lower BE, which indicates a high contamination of  $\text{OH}^-$  species despite the experimental precautions taken to avoid the hydration of the samples (see Experimental). This effect is especially important for the sample exposed to air for several days, where the peak associated with  $\text{OH}^-$  species has dramatically increased, while that due to  $\text{O}^{2-}$  ions has almost disappeared.

The high reactivity of  $\text{YBa}_2\text{Cu}_3\text{O}_{7-x}$  with water can be attributed (20) not only to the high hydration energy of  $\text{Ba}^{2+}$  ions but also to the existence of  $\text{O}^-$  and/or  $\text{O}_2^{2-}$  lattice species which are extremely reactive. In fact, these species are responsible for the spontaneous release of molecular oxygen from the superconductor's lattice when put in contact with water, probably according to the reactions (20)

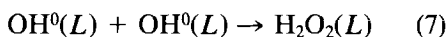


where  $(L)$  represents lattice species.

Both reactions should involve the generation of  $\text{H}_2\text{O}_2$  molecules, which further decompose into oxygen and water, a reaction which is catalyzed by  $\text{Cu}^{2+}(L)$  ions:



The same should be valid for  $\text{O}^-(L)$  species through the generation of more stable  $\text{OH}^0$  radicals from which  $\text{H}_2\text{O}_2$  is formed:



During reactions (2) and (3) the lattice loses two negative charges; charge neutrality is preserved because  $\text{O}^-$  vacancies in the  $\text{Cu}_1\text{-O}$  chains are filled by  $\text{OH}^-$  ions, which become very strongly coordinated to  $\text{Ba}^{2+}$  lattice ions. Consequently, the chemical bonds between  $\text{Cu}_1$  and  $\text{OH}^-$  groups are broken and the solid decomposes to give  $\text{Ba}(\text{OH})_2$ ,  $\text{CuO}$ , and semiconducting  $\text{Y}_2\text{BaCuO}_5$  (26).

The identification of  $\text{O}^-$  and/or  $\text{O}_2^{2-}$  species in the  $\text{O}_{1s}$  spectrum of superconducting  $\text{YBa}_2\text{Cu}_3\text{O}_{6.9}$  is ambiguous because of the presence of a strong signal due to  $\text{OH}^-$  ions at a BE very close to that of  $\text{O}^-$  (25). In

fact, the  $\text{O}_{1s}$  spectra of 4- $\text{N}_2$  and 8- $\text{N}_2$  samples, which should not contain  $\text{O}^-$  species, are very similar to those of the superconducting sample, 4- $\text{O}_2$ . Gourieux *et al.* (27) compared the spectra corresponding to clean surfaces, obtained by scrambling *in situ* samples of composition  $\text{YBa}_2\text{Cu}_3\text{O}_{6.76}$ , with the spectra of the same samples highly contaminated, and claimed to be able to distinguish a peak at  $\text{BE} \approx 532$  eV due to contaminants ( $\text{OH}^-$  probably) from another peak at 530–531 eV due to singly charged oxygen species (probably  $\text{O}^-$  and/or  $\text{O}_2^{2-}$ ). However, these results must be taken cautiously because of the difficulties in obtaining fully water-free surfaces, even under the experimental conditions used by Gourieux *et al.*

On the other hand, the peak corresponding to  $\text{OH}^-$  species in the most reduced sample,  $\text{YBa}_2\text{Cu}_3\text{O}_{6.1}$ , shows a clear asymmetry toward higher BE due to the presence of a weak component, which may be attributed to water molecules nondissociatively adsorbed on  $\text{Cu}^+(L)$  ions. Typical  $\text{O}_{1s}$  spectra of hydrogen-bonded water molecules show in fact one peak at BE between 533 and 535 eV (25, 27).

Figure 3 shows the  $\text{Ba}_{3d}$  spectra for the various samples used in this study. Two well-differentiated spectral features can be observed in the highly hydroxylated sample. The very intense peak centered at about 781 eV should correspond to the  $\text{Ba}_{3d_{5/2}}$  signal of the  $\text{Ba}(\text{OH})_2$  phase formed during the decomposition of the superconductor by reaction with water (26). The small shoulder between 777 and 778 eV must be associated with  $\text{Ba}^{2+}$  ions coordinated to  $\text{O}^{2-}$  species in the superconductor's lattice. The spectra corresponding to the samples 4- $\text{O}_2$  ( $x \approx 0.1$ ) and 4- $\text{N}_2$  ( $x \approx 0.4$ ) are very similar and show a peak centered at  $\sim 779$  eV, which suggests the existence of only one type of  $\text{Ba}^{2+}$  ions (those present in the superconductor) and, therefore, the absence of the  $\text{Ba}(\text{OH})_2$  phase. It

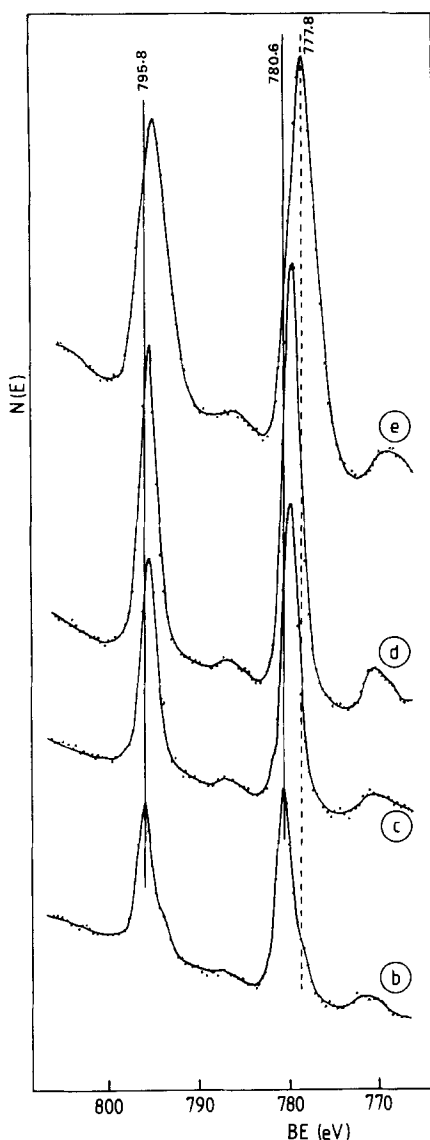


FIG. 3. Room-temperature XPS  $\text{Ba}_{4d}$  core-level spectra of the  $\text{YBa}_2\text{Cu}_3\text{O}_{7-x}$  sample subjected to the same pretreatments as in Fig. 1. All the spectra again show whole spin-orbit splitting.

is worth noting that in the most reduced sample ( $x = 0.9$ ) the  $\text{Ba}_{3d_{5/2}}$  signal appears shifted toward lower BE by about 1 eV. A possible reason for this is the drastic changes occurring in the lattice positions surrounding the Ba ions. These changes

mainly concern the  $\text{Cu}_1\text{-O}$  chains parallel to the  $b$  axis. In fact, for low values of  $x$  (superconducting sample) Ba ions are screened by  $\text{O}^-$  species in those chains. However, when  $x$  increases these species are lost, divalent  $\text{Cu}_1$  ions are reduced to  $\text{Cu}^+$  and the screening effect disappears.

### Conclusions

The room-temperature XPS study of the  $\text{YBa}_2\text{Cu}_3\text{O}_{7-x}$  compound for different values of  $x$  ( $0.9 \geq x \geq 0.1$ ) shows that the copper ground-state electronic configuration for  $x \approx 0.1$  (superconducting composition) is not  $3d^8$  but rather  $3d^9KL$ , where  $K$  represents an electron of the conduction band and  $L$  stands for a hole in the oxygen bonded to a virtually divalent copper. Therefore, one can reasonably assume a strong  $\text{Cu}^{2+}\text{-O}^-$  hybridization in the superconducting sample. As  $x$  increases the amount of monovalent copper ( $3d^{10}$  ground-state configuration) is found to increase. It can be assumed that, under sample reduction,  $\text{O}^-$  species from  $\text{Cu}_1\text{-O}$  chains parallel to the crystallographic  $b$  axis leave the lattice, electrons being transferred to adjacent  $\text{Cu}^{2+}$  ions. For  $x \approx 0.9$  the amount of  $\text{Cu}^+$  clearly predominates over that of  $\text{Cu}^{2+}$ .

The special features of the  $\text{O}_{1s}$  core-level spectra show the high reactivity of the superconducting material with water vapor from the air. The XPS signal due to adsorbed  $\text{OH}^-$  species is higher than that of  $\text{O}^{2-}$  lattice ions, even if precautions are taken in order to avoid sample contamination. These results are consistent with the existence of delocalized holes in  $\text{O}_{2p}$  orbitals.  $\text{O}^-$  lattice species strongly react with  $\text{H}_2\text{O}$  molecules producing  $\text{OH}^0$  radicals ( $\text{O}^-(L) + \text{H}_2\text{O} \rightarrow \text{OH}^0(L) + \text{OH}^-$ ), which further recombine to generate more stable  $\text{H}_2\text{O}_2$  species. Lattice  $\text{Cu}^{2+}$  ions then catalyze  $\text{H}_2\text{O}_2$  decomposition and molecular oxygen is evolved. In order to preserve charge neutrality  $\text{O}^-$  vacancies are filled by



OH<sup>-</sup> ions from water molecules. These OH<sup>-</sup> groups become preferentially coordinated to Ba<sup>2+</sup> ions as inferred from the Ba<sub>3d</sub> XPS spectrum. Consequently, chemical bonds between Cu<sub>1</sub> and OH<sup>-</sup> groups are broken and the solid decomposes.

## References

1. See, for instance, T. SIEGRIST, S. SUNSHINE, D. W. MURPHY, R. I. CAVA, AND S. M. ZAHNVOK, *Phys. Rev. B* **35**, 7137 (1987); R. M. HAZENB, L. W. FINGER, R. J. ANGEL, C. T. PREWITT, N. L. ROSS, H. K. MAO, AND C. G. ADIDIACOS, *Phys. Rev. B* **35**, 7238 (1987); L. F. SCHNEEMEYER, J. V. WASZCZAK, T. SIEGRIST, R. B. VAN DORER, L. W. RUPP, B. BATLOGG, R. J. CAVA, AND D. W. MURPHY, *Nature (London)* **328**, 601 (1987).
2. See, for instance, J. J. CAPPONI, C. CHAILLONT, A. W. HEWAT, P. LIJAY, M. MAREZIO, N. NGUYEN, B. RAVEAU, J. L. SOUBEYROUX, J. L. THOLEUCE, AND R. TORUNIER, *Europhys. Lett* **3**, 1301 (1987); T. KAJITANI, K. OH-ISHI, M. KIKUCHI, Y. SYONO, AND M. HIBABAYASHI, *Japan. J. Appl. Phys. L* **26**, 1144 (1987); S. KATANO, S. FUNAHASHI, T. HATANO, A. MATSUSHITA, K. NAKAMURA, T. MATSUMOTO, AND K. OGAWA, *Japan. J. Appl. Phys. L* **26**, 1046 (1987); W. I. F. DAVID, W. T. A. HARRISON, J. M. F. GUNN, O. MOZÉ, A. K. SOPER, P. DAY, J. D. JORGENSEN, D. G. HINKS, M. A. BENO, L. SODERHOLM, D. W. CAPONE II, I. K. SCHULLER, C. U. SEGRE, K. THANK, AND J. D. GRACE, *Nature (London)* **327**, 310 (1987).
3. G. VAN TENDELOO, H. W. ZANDBERGEN, T. OKABE, AND S. AMELIUKS, *Solid State Commun.* **63**, 969 (1987); M. HERVIEU, B. DOMENGES, C. MICHEL, AND B. RAVEAU, *Europhys. Lett.* **4**, 205 (1987).
4. Y. JEON, F. LU, H. JHANS, S. A. SHAHEEN, G. LIANG, M. CROFT, P. H. ANSARI, K. V. RAMANUJACHARY, E. A. HAYRI, S. PI FINE, S. LI, X. H. FEUG, M. GREENBLATT, L. H. GREENE AND J. M. TARASCON, *Phys. Rev. B* **36**, 3891 (1987).
5. F. BAUDELEF, G. COLLIN, E. DARTYGE, A. FONTAINE, J. P. KAPPLER, G. KRILL, J. P. ITIE, J. JEGONDEZ, M. MAURER, PH. MONOD, A. REVCOLEVSKI, H. TOLENTINI, G. TOURILLON, AND M. VERDAGUER, *Z. Phys. B* **69**, 149 (1987).
6. H. OYANAGI, H. IHARA, T. MATSUBURA, M. TOKUMOTO, T. MATSUSHITA, M. HIRABAYASHI, K. MURATA, N. TERADA, T. YAO, H. IWASAKI, AND Y. KIMURA, *Japan. J. Appl. Phys. L* **26**, 1561 (1987).
7. A. BIANCONI, A. COUGIN CASTELLANO, M. DE SANTIS, P. RUDOLF, P. LEGARDE, A. M. FLANK, AND A. MARCELLI, *Solid. State. Commun.* **63**, 1009 (1987).
8. S. HORN, J. COVI, S. A. SHAHEEN, Y. JEON, M. CROFT, C. L. CHANG, AND M. L. DEN BOER, *Phys. Rev. B* **36**, 3895 (1987).
9. G. M. ANTONINI, C. CALANDRA, F. CORNI, F. D. MATA COTTA, AND M. SACCI, *Europhys. Lett* **4**, 851 (1987).
10. J. B. BOYCE, F. BRIDGES, T. CLAESON, R. S. HOWLAND, AND R. H. GEBALLE, *Phys. Rev. B* **36**, 5251 (1987).
11. B. LENGELER, M. WILHELM, B. JOBST, W. SEHWAEN, B. SEEBAHER, AND U. HILLEBRECHT, *Solid. State. Commun.* **65**, 1545 (1988).
12. N. G. STOFFEL, J. M. TARASCON, Y. CHANG, M. ONELLION, D. W. NILES, AND G. MARGARITONDO, *Phys. Rev. B* **36**, 3986 (1987).
13. A. BIANCONI, A. C. CASTELLANO, M. DE SANTIN, P. DELOGU, A. GARGANO, AND R. GIORGI, *Solid. State. Commun.* **63**, 1135 (1987).
14. P. STEINER, S. HÜFNER, V. KINSINGER, I. SANDER, B. SIEGWART, M. SCHMITT, R. SCHULZ, S. JUNK, G. SCHWITZGEBEL, A. GOLD, C. POLITIS, H. P. MÜLLER, R. HOPPE, S. KEMMLER-SACK, AND C. KUNZ, *Z. Phys. B* **69**, 449 (1988).
15. J. A. YARMOFF, D. R. CLARKE, W. DRUBE, U. O. KARLSSON, A. T. IBRAHIMI, AND F. J. HIMPEL, *Phys. Rev. B* **36**, 3964 (1987).
16. N. NÜCKER, J. FINK, J. C. FUGGLE, P. J. DURHAM, AND W. M. TEMMERMAN, *Phys. Rev. B* **37**, 5158 (1988).
17. J. A. YARMOFF *et al.* *Phys. Rev. B* **36**, 3967 (1987).
18. K. KAMARAS, C. D. PORTER, M. G. DOSS, S. L. HERR, AND D. B. TARNER, *Phys. Rev. Lett.* **59**, 919 (1987).
19. P. STEINER, V. KINSINGER, I. SANDER, B. SIEGWART, S. HÜFNER, C. POLITIS, R. HOPE, AND H. P. MÜLLER, *Z. Phys. B* **67**, 497 (1987).
20. P. SALVADOR, E. FERNÁNDEZ-SÁNCHEZ, J. A. GARCÍA-DOMÍNGUEZ, J. AMADOR, C. CASCALES, AND I. RASINES, *Solid State. Commun.* **70**, 71 (1989).
21. P. SALVADOR *et al.*, unpublished results.
22. A. MANTHIRAM, J. S. SWINNEA, Z. T. SUI, H. STEINFINK, AND J. B. GOODENOUGH, *J. Amer. Chem. Soc.* **109**, 6667 (1987).
23. G. PANZER, B. ERGET, AND H. P. SCHMIDT, *Surf. Sci.* **151**, 400 (1985).
24. S. HUFNER, *Solid. State. Commun.* **47**, 943 (1983); G. VAN DER LAAN, C. WESTRA, C. HAAS, AND G. A. SAWATSKY, *Phys. Rev. B* **23**, 4369 (1981).
25. L. M. MORONEY, R. S. SMART, AND M. W. ROBERTS, *J. Chem. Soc. Faraday Trans. T* **79**,

- 1769 (1983); P. A. THIEL, *Surf. Sci. Rep.* **7**, 211 (1987); M. S. BARTEAU AND R. J. MADIX, *Surf. Sci.* **140**, 108 (1985).
26. M. F. YAN, R. L. BARNES, H. M. O'BRYAN, JR., P. K. GALLAGHER, R. C. SHERWOOD, AND S. JIN, *Appl. Phys. Lett* **57**, 532 (1987).
27. T. GOURIEUX, G. KRILL, M. MAURER, M. F. RAVET, A. MENNY, H. TOLENTINO, AND A. FONTAINE, *Phys. Rev. B* **37**, 7516 (1988).
28. J. FUGGLE, L. M. WATSON, D. J. FABIAN, AND S. AFFROSSMAN, *Surf. Sci.* **49**, 61 (1979); S. L. AIU, M. W. RUCKMAN, N. B. BROOKES, P. D. JOHNSON, J. CHEN, C. L. LIN, AND M. STROUGIN, *Phys. Rev. B* **37**, 3747 (1988).